Condensation reaction vs. ligand exchange with first-row transition metal cations: a theoretical study of Cu$^+$ heteroleptic model complexes

Sophie Le Caër, Hélène Mestdagh, Philippe Maître[*]

Laboratoire de Chimie Physique (UMR 8000-CNRS), Université de Paris XI-Bâtiment 350, Orsay Cedex 91405, France

Abstract

Analysis of the evolution of the binding energy to a late first-row transition metal cation M$^+$ shows that the third ligand is significantly less strongly bound than the two first. The present study suggests that a new type of cluster-assisted reactions could be induced by the metal center when it is tri-coordinated. Cu$^+$ complexes have been chosen as models for the quantum chemical calculations (density functional and post-Hartree–Fock ab initio). First, an emphasis is made on the analysis of the evolution of the binding energy as the coordination number n varies from 1 to 4 in Cu$^+$(H$_2$O)$_n$ and Cu$^+$(CO)$_n$. The evolution of the electronic repulsion between the σ donating orbitals of the ligands and the 3d orbitals is discussed in details. Second, we consider the successive substitution reactions of CO by H$_2$O ligand from Cu$^+$(CO)$_n$ ($n = 1$–4). Our calculations suggest that rather than the simple substitution reaction of CO by ROR$'$ (R, R$'$ = H, alkyl), formation of an acid or ester could occur in the coordination sphere of the metal. Whereas kinetics is likely to be unfavorable in the case of Cu$^+$, such condensation reaction of ROR$'$ and CO could be observed with late first-row transition metal cations such as Fe$^+$.
© 2003 Elsevier Science B.V. All rights reserved.

Keywords: Condensation reaction; Ligand exchange; Transition metal

1. Introduction

Gas phase study of transition metal ions has been shown to provide valuable informations to better understand the interaction of a transition metal atom with its environment [1,2]. The synergism between experiment and quantum chemistry has been essential for the development of this field [3–8]. Systematic studies of the interaction of a ligand L with a series of transition metal cations M$^+$ help to appreciate the relative extent of the electrostatic and charge transfer involved in the M$^+$–L bond. Binding energies and entropies have also been measured for the successive attachment of several ligands to M$^+$ [6], offering an understanding of the competition between direct coordination to the metal and formation of the second coordination sphere. In this context, the analysis of the evolution of the M$^+$–L bonding as a function of the coordination of the metal center was also important to evaluate the relative extent of the ligand–ligand

---
* Corresponding author. Tel.: +33-1-69-15-74-63;
fax: +33-1-69-15-30-53.
E-mail address: philippe.maitre@lcp.u-psud.fr (P. Maître).

repulsion and more subtle electronic factors. Among these factors, polarization of the transition metal cation has been shown to be essential [3].

This work is part of an ongoing study of mechanistic and thermochemical aspects of the gas phase reactivity of Fe^+ complexes. For example, successive substitution reactions of CO ligands from $Fe^+(CO)_n$ complexes by water [9], methanol [10] and dimethyl-ether [11] have been studied. This work may provide interesting informations on the thermochemistry of heteroleptic complexes which have been less studied than the homoleptic ones. The study of the successive displacements of CO ligands from $Fe^+(CO)_n$ reveals that the behavior of mono- and di-coordinated complexes, $Fe^+(CO)_1$ and $Fe^+(CO)_2$, is very different from the one of tri-coordinated and up complexes. For instance, the complete substitution of the CO ligands of $Fe^+(CO)_{1-2}$ by $L = H_2O$, CH_3OH and CH_3OCH_3 is observed, whereas one CO remains always unsubstituted when the reactant ion is $Fe^+(CO)_3$ or $Fe^+(CO)_4$. This behavior could owe its origin to a change of the relative strength of CO and oxygen-donor ligand with Fe^+ as a function of the substitution reactions. Reactivity could also be invoked and one might think that the remaining CO ligand has been activated leading to the formation of an acid or ester molecule in the coordination sphere of the transition metal. We believe that such reactivity in tri- or tetra-coordinated complexes could find its origin in the significant drop of the binding energy to Fe^+ after the addition of the second ligand. This could be generalized to all the late first-row transition metal cations: the binding energy of the third and fourth ligands being relatively small, a condensation reaction like the formation of acid from CO and ROH ($R = H$, CH_3) could become favorable, since the loss in binding energy to the metal cation would be balanced by the intrinsic exothermicity of the reaction assisted by the metal center.

This paper aims at evaluating the two possible interpretations. Heteroleptic complexes of Cu^+, where the ligands are CO and H_2O, have been chosen as prototype complexes of late first-row transition metal cations. Only thermodynamic aspects have been studied in this case since energy barriers are expected to be quite high in energy for a closed-shell d^{10} Cu^+ ion. A theoretical investigation of the potential energy surfaces associated to the reaction of methanoic acid (HCOOH) formation from $H_2O + CO$ assisted by Fe^+ is under study. It should be noted that the trends in the thermodynamics of the reactions in the case of Fe^+ parallel those of Cu^+ presented here, suggesting that Cu^+ is a good representative of late first-row transition metal cations.

2. Quantum chemical methods

Both density functional theory (DFT) and post-Hartree–Fock ab initio approaches have been used. In conjunction with the DFT approach, two basis sets, denoted as Basis1 and Basis2, have been employed. In Basis1, Cu is described by an [8s6p4d1f] contraction of the (14s11p6d3f) primitive set of Wachters [12] supplemented by two diffuse p functions, a diffuse d function ($\alpha = 0.1491$) and a contraction of three f functions [13]. Ligands are described by a polarized double-zeta basis set [14], the exponent of the polarized functions being $\alpha_p(H) = 1.0$, $\alpha_d(C) = 0.75$, $\alpha_d(O) = 0.85$. In Basis2, the ligand basis set consists of the standard 6-311G, complemented by a set of diffuse sp functions, two d polarization sets for heavy atoms, and two p polarization functions for H [15]. The Cu set is a [9s6p4d2f] contraction of the (15s11p6d2f) primitive set. That is, from Basis1, a diffuse s ($\alpha = 0.0123$) and two f polarization ($\alpha = 2.88$ and 0.72) are added.

Basis2 has also been used at the post-Hartree–Fock ab initio levels, as well as larger basis sets consisting of augmented correlation consistent basis sets (aug-cc-pVDZ, aug-cc-pVTZ, and aug-cc-pVQZ, hereafter denoted as AVDZ, AVTZ and AVQZ, respectively) for the ligands [16], and an atomic natural contraction proposed by Bauschlicher [13] for Cu.

Hybrid density functional B3LYP [17] has been used in conjunction with Basis1 to characterize the geometries of the complexes, and the corresponding harmonic vibrational frequencies were used throughout

this work. Basis2, larger basis including diffuse functions on the ligands, has been used to derive the energetics at the B3LYP level, which has been shown to be well adapted to describing transition metal complexes [18]. Nevertheless, whereas the geometries and harmonic vibrational frequencies [19] are very accurate, the energetics derived at this level still need further calibration. Post-Hartree–Fock ab initio calculations using the B3LYP/Basis1 optimized geometries have been performed. Only the valence electrons are correlated at this level. For small clusters, the restricted coupled cluster of singles and doubles [20] including a perturbational treatment of connected triples [21], RCCSD(T), has been used. In the case of $Cu^+(CO)_n$ complexes, relativistic corrections were evaluated by computing expectation values of the mass-velocity and 1-electron Darwin integrals using the Cowan-Griffin approach as implemented in MOLPRO [22]. Larger clusters were only treated at the MP2 level.

B3LYP calculations were performed using Gaussian 98 [23] and MOLPRO [22] was used for the post-Hartree–Fock MP2 and RCCSD(T) ones.

3. Homoleptic complexes

3.1. $Cu^+(H_2O)_n$ (n = 1–4) clusters

Hydrated clusters of $Cu(H_2O)_n^+$ have been studied experimentally [24,25] and theoretically [26–29]. Magnera et al. [24], and later on, Armentrout's group [25], reported gas phase incremental binding energies for $n = 1$–4 clusters using collision induced dissociation (CID) techniques. The second binding energy was found to be stronger than the first by 4 kcal/mol, while the third and fourth water molecules were found to be significantly less strongly bound than the two first. In the first theoretical investigation of the $Cu(H_2O)_n^+$ clusters, Rosi and Bauschlicher [26] provided an interpretation for the evolution of the binding energy as a function of the cluster size. They found a significant polarization of Cu^+, due to an sd hybridization, associated to the addition of the first water. It was shown that this polarization paid by the first ligand, also bene-
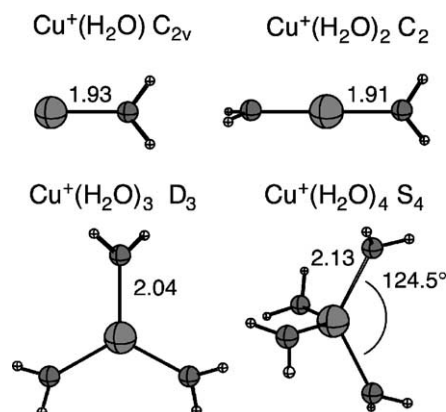

Fig. 1. Optimized structures of $Cu^+(H_2O)$, $Cu^+(H_2O)_2$, $Cu^+(H_2O)_3$ and $Cu^+(H_2O)_4$ complexes. Only the essential geometrical parameters are given (distances in angstroms and angles in degrees). The $Cu^+(H_2O)_2$ C_2 minimum is a slightly distorted D_{2d} structure. Similarly, $Cu^+(H_2O)_3$ and $Cu^+(H_2O)_4$ minima derived from a slight distortion from the D_3 and S_4 given structures, respectively (see text).

fits to the second ligand, thus offering an interpretation for the second water molecule being more strongly bound than the first one. Then, about two-third of the binding energy between the second and the third ligand was found to be due to ligand–ligand repulsion and one-third to an increase of the metal–ligand repulsion resulting from a loss of sd hybridization.

B3LYP/Basis1 optimized geometries of the Cu^+ $(H_2O)_n$ clusters are given in Fig. 1. As discussed by Feller et al. [29], the nature of the stationary point may vary with the level of electronic correlation treatment. For instance, they found that the nature of the $Cu^+(H_2O)_2$ (D_{2d}) stationary point is a minimum at the Hartree–Fock level, while this structure is characterized by a doubly degenerate imaginary frequency of i150 cm^{-1} at the MP2 level, the corresponding normal mode being a combination of O–Cu–O bending and water twisting modes leading to a C_2 global minimum at the MP2 level [29]. Interestingly, it seems that the topology of the potential energy surface of $Cu^+(H_2O)_2$ is similar at the MP2 and B3LYP levels. Indeed, $Cu^+(H_2O)_2$ (D_{2d}) was also found to present a doubly degenerate imaginary frequency of i36 cm^{-1} at the B3LYP level. As already found by

Feller et al., the energetic stabilization associated to the $D_{2d} \rightarrow C_2$ distortion is very small (only 4×10^{-5} a.u. at the B3LYP level). Similarly, the D_3 highly symmetric structure for $Cu^+(H_2O)_3$ and the S_4 one for $Cu^+(H_2O)_4$ were found to present a very small imaginary frequency (doubly degenerate i64 cm^{-1} for $Cu^+(H_2O)_3$ and i36 cm^{-1} for $Cu^+(H_2O)_4$). As shown by Feller et al., the absolute minimum for these two clusters correspond to a structure where one and two water molecules, respectively are in the second coordination shell of Cu^+. Nevertheless, we are here only interested in structures with direct coordination of the water molecules to Cu^+ in order to modelize the common trend observed experimentally for the reactions of $Fe(CO)_n^+$ with water, methanol and dimethylether. Following the imaginary mode of the highly symmetric structures, secondary minima where all the water molecules are in the first solvation shell of Cu^+ have been located at the B3LYP level for $Cu^+(H_2O)_3$ and $Cu^+(H_2O)_4$. They both present a C_2 symmetry and are very similar to the one proposed by Feller et al. As also found by these authors, they are only slightly lower in energy than the corresponding highly symmetric structures. Thus, in order to keep the large ab initio calculations tractable, highly symmetric structure for $Cu^+(H_2O)_2$ (D_{2d}), $Cu^+(H_2O)_3$ (D_3) and $Cu^+(H_2O)_4$ (S_4) were used for the large ab initio calculations since they only present a very small imaginary frequency (doubly degenerate i64 cm^{-1} for $Cu^+(H_2O)_3$ and i36 cm^{-1} for $Cu^+(H_2O)_4$).

Overall, as found by other authors, the evolution of the Cu–O distance, larger in $Cu^+(H_2O)_{3-4}$ than in $Cu^+(H_2O)_{1-2}$, is consistent with the evolution of the binding energy. As expected, since electronic correlation is known to reinforce the M^+–ligand bonding, our B3LYP bond lengths are smaller by 0.01 Å, than the ones determined at the Hartree–Fock level [28]. In the case of $Cu^+(H_2O)_1$ and $Cu^+(H_2O)_2$, comparison can also be made with the RCCSD(T)/aug-cc-pVQZ and RCCSD(T)/aug-cc-pVTZ optimized geometries, respectively [29]. It is interesting to note that our B3LYP/Basis1 Cu–O bond lengths (1.93 and 1.91 Å) are in excellent agreement with the one of Feller et al. [29]. This comparison shows that for water containing clusters, the B3LYP/Basis1 geometries are reliable and that geometry reoptimization at higher level would not significantly improve the description of these complexes.

Binding energies are reported in Table 1. Our calculated values are given along with the experimental [25] and calculated values [28,29]. It should be noted that, for a purpose of comparison, values given from [29] correspond to the highest theoretical level for the structure where all the water molecules lie in the first solvation shell of Cu^+. As can be seen in this table, the main features of the evolution of the binding energy are correctly reproduced at all levels of theory, except at the B3LYP in the smallest basis set (Basis1) where BDEs are overestimated. Part of it may be attributed to the basis set superposition error (BSSE) which has been estimated to range from 2.4 to 2.6 kcal/mol at this level using the counterpoise method. Extending the basis set to Basis2, which includes diffuse functions on the ligands, significantly reduces the BSSE, which

Table 1
Summary of 0 K values for $D_0[(H_2O)_{n-1}Cu^+-H_2O]$

	B3LYP/Basis1	B3LYP/Basis2	MP2/Basis2	MP2 AvxZ (x = V/T/Q)	Exp. [25]	[29][a]	[28][b]
Cu^+-OH_2	45.9	40.7	38.0	36.2/38.3/38.7	35.8–39.4	41.0	38.8
$(H_2O)Cu^+-OH_2$	45.0	40.2	40.2	38.0/40.2/40.7	39.0–42.2	45.7	39.4
$(H_2O)_2Cu^+-OH_2$	15.4	12.2	11.7	13.1/12.0	11.8–15.4	14.8	15.4
$(H_2O)_3Cu^+-OH_2$	11.8	9.1	10.1	10.6/9.8	12.0–14.0	9.2	13.3

All values are in kcal/mol.

[a] D_e values. For n = 1, 2: RCCSD(T) method with estimated complete basis set. For n = 3, 4: MP2 method (with all the ligands directly bound to Cu).

[b] MCPF method.

ranges from 0.8 to 1.1 kcal/mol, and brings the two first B3LYP/Basis2 binding energies in better agreement with the experimental values. The experimentally observed slight increase of the binding energy from the first to the second ligand is not reproduced at the B3LYP level. This behavior might be attributed to the fact that B3LYP systematically overestimates the first binding energy to a transition metal cation [30]. Nevertheless, in comparison with the experiments and with other calculations, the trends in the evolution of the binding energy are correctly reproduced at the B3LYP/Basis2 level, in particular the drop in the binding energy associated to the attachment of the third ligand.

Binding energies at the MP2 level using the B3LYP/Basis1 optimized geometries are also reported in Table 1. Compared to B3LYP, MP2 provides a better description of the two first complexes, the second binding energy being predicted larger than the first as found experimentally. Nevertheless, the main weakness of B3LYP, i.e., underestimation of the fourth BDE, is also found at the MP2 level.

3.2. $Cu^+(CO)_n$ (n = 1–4) clusters

The successive binding energies of $Cu(CO)_n{}^+$ complexes have been determined experimentally for $n = 1$–4 [31] but only the two first complexes have been studied theoretically [32]. As for the water clusters, an increase of the binding energy has been observed from the first to the second ligand (35.6 and 41.1 kcal/mol, respectively), the third and the fourth BDE (17.9 and 12.7 kcal/mol, respectively) being significantly smaller than the two first ones [31]. Contrary to the case of the water clusters where Rosi and Bauschlicher showed that the bonding is essentially electrostatic [28], the bonding of CO to a transition metal is known to involve a double charge transfer. Interestingly, whereas the bonding in these two systems are very different, the evolution of the binding energy with respect to the size of the cluster is very similar. Moreover, the sum of the four binding energies derived by Armentrout and co-workers [31] is also of the same order: 104.8
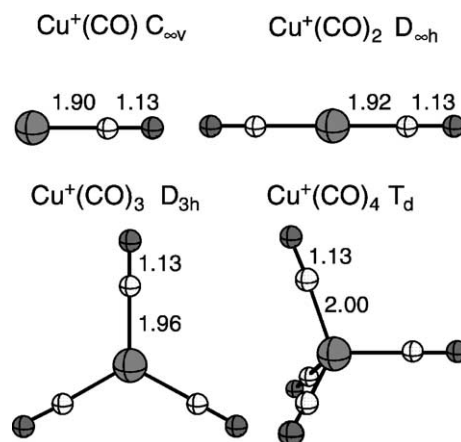

Fig. 2. Complexes of $Cu^+(CO)$, $Cu^+(CO)_2$, $Cu^+(CO)_3$ and $Cu^+(CO)_4$. Distances are given in angstroms and angles in degrees.

and 107.3 kcal/mol for water and carbonyl clusters, respectively.

B3LYP/Basis1 optimized geometries of the $Cu^+(CO)_n$ clusters are given in Fig. 2. Compared to the optimized geometries obtained at the MCPF level including relativistic effects [32], the Cu^+–CO distance is significantly shorter (0.04 Å) in the case of $Cu^+(CO)_1$, but the Cu^+–CO distance in the second cluster is only 0.01 Å shorter than the one of Bauschlicher. The larger discrepancy for the first cluster might be related to the fact that the first BDE is systematically overestimated at the B3LYP level [30]. As for the water clusters, one observes a significant lengthening of the metal–ligand distance with the addition of the third and fourth ligands.

The calculated binding energies of $Cu^+(CO)_n$ clusters are reported in Table 2. As compared to the experimental results, the B3LYP approach provides the same trends as in the case of the water clusters. That is, using the small basis set (B3LYP/Basis1), one overestimates the binding energies, and especially the first one (see Table 2). Using the larger basis set (B3LYP/Basis2), B3LYP provides a good approach for the description of the successive binding energies. As can be seen in Table 2, the MP2 approach does not provide an interesting alternative since it systematically overestimates the third and fourth binding

Table 2
Summary of 0 K values for $D_0[(CO)_{n-1}Cu^+-CO]$

	B3LYP/Basis1	B3LYP/Basis2	MP2/Basis2	MP2 AvxZ (x = V/T/Q)	RCCSD(T)[a]	[31]	[32]
Cu^+-CO	40.7	37.1	33.5	32.7/35.9/36.2	28.4/31.4/31.8	33.9–37.3	32.1
$(CO)Cu^+-CO$	40.8	36.5	38.3	38.4/40.2/40.5	33.2/34.6/*34.5*	40.4–41.8	32.5
$(CO)_2Cu^+-CO$	20.5	16.6	22.5	21.4/22.4	18.0/*18.3*	16.9–18.9	
$(CO)_3Cu^+-CO$	15.7	13.4	19.1	19.1/19.2	15.2/*14.2*	12.0–13.4	

All values are in kcal/mol.

[a] The values in italics correspond to RCCSD(T) energies determined using the triple contribution calculated without diffuse functions.

energies by about 4 and 6 kcal/mol, respectively. A similar observation had been made by Ricca and Bauschlicher in the case of $Fe^+(CO)_{1-5}$ clusters, the fifth binding energy being too large [30].

In the following sections, we are interested in the heteroleptic complexes of Cu^+ for which there is no experimental data. Nevertheless, one can expect that the performances of a given approach would be the same as in the homoleptic $Cu^+(H_2O)_n$ and $Cu^+(CO)_n$ complexes. Since we are especially interested in the chemistry of tri-coordinated and up complexes, it seems that the B3LYP approach is more adequate since in the case of $Cu^+(CO)_n$ complexes, MP2 significantly overestimates the binding energies of the third and fourth ligands to the metal cation. Considering the poor performances of MP2 for describing the energetics of the addition of the third and fourth ligands, RCCSD(T) calculations have been performed using the large ANO bases.

The corresponding binding energies are reported in Table 2. In the case of $Cu^+(CO)$, RCCSD(T) binding energy increases with the size of the basis set, and the calculation in the largest basis set leads to a BDE value of 31.8 kcal/mol. Considering the convergence of the binding energy with the basis set, an estimation of the complete basis set (CBS) value can be reached using the two-point extrapolation formulae proposed by Martin [33] and gives D_e = 33.4 kcal/mol, leading to a 0 K BDE value of 32.0 kcal/mol. For the largest calculations, we were unable to directly determine the effect of the triples excitations. Therefore, since the diffuse functions are not expected to play a role in the correlation energy of the valence electrons, RCCSD(T) binding energies in italics in Table 2 have

been evaluated adding the energetics contribution of the triples without diffuse functions to the RCCSD energy determined with diffuse functions. The second binding energy was predicted to be 34.5 kcal/mol using the largest basis set (see Table 2). This value is larger than the first BDE in agreement with the experimental values. RCCSD(T) energies could not be determined in the largest basis set (AVQZ) for the third and fourth complexes. Using the AVTZ on the ligands, and estimating the contribution of the triple excitations in the VTZ basis, binding energies of 18.3 and 14.2 kcal/mol have been determined for the third and fourth binding energies, respectively (see Table 2). It has been shown that within the neglected effects, the differential core–valence correlation energy and the relativistic effects have a non-negligible contribution to the binding energies [34]. Relativistic effects have been estimated at the Hartree–Fock levels using the AVDZ on the ligands. The corresponding contribution to the four successive binding energies amounts to 3, 3, 0.4 and 0.5 kcal/mol. This strong relativistic contribution for the two first binding energy is a typical signature of the donation from the carbonyl to the metal 4s orbital. The smaller contribution to the third and fourth binding energies is not surprising since the donation of the metal 4s decreases as the binding energy after the addition of the third ligand. Similarly, the core–valence contribution is expected to be larger for the first two binding energies than for the third and fourth. Unfortunately, the size of the systems prevents for the determination of core–valence correlation. Core–valence contribution have been calculated in the case of neutral FeCO complex and a similar increase was assumed for the (CO)Fe–CO bond [34]. This correlation energy

increases the Fe–CO binding energy by 2.3 kcal/mol. As a conclusion, these estimated values for the contribution of the differential core–valence correlation energy and the relativistic effects would bring the first and second binding energies in good agreement with experiment, but the third and fourth BDE would range in the upper limits of the experimental values.

4. Heteroleptic complexes of $Cu^+(CO)_n(H_2O)_m$, $1 \leq n \leq 3$, $1 \leq m \leq 3$, $n+m \leq 4$

The geometries of the $Cu^+(CO)_n(H_2O)_m$ heteroleptic complexes are given in Fig. 3. All the structures correspond to a minimum. Binding energies of CO and H_2O at the B3LYP/Basis2 level of theory in these complexes are reported in Table 3. Binding energies in homoleptic complexes are also given for comparison.

The di-coordinated $Cu^+(CO)(H_2O)$ complex presents a C_{2v} symmetry. As can be seen in Table 3, the binding energy is enhanced in this heteroleptic complex as compared to the homoleptic ones. That is, the CO binding to $Cu^+(H_2O)$ (39.7 kcal/mol) is greater than the binding energy to $Cu^+(CO)$ (36.5 kcal/mol).

Table 3
Binding energies (kcal/mol) evaluated at the B3LYP/Basis2 level

	BDE
$(CO)Cu^+$–CO	36.5
$(H_2O)Cu^+$–CO	39.7
$(CO)_2Cu^+$–CO	16.6
$(H_2O)(CO)Cu^+$–CO	14.8
$(H_2O)_2Cu^+$–CO	16.9
$(H_2O)Cu^+$–H_2O	40.2
$(CO)Cu^+$–H_2O	43.3
$(H_2O)_2Cu^+$–H_2O	12.2
$(H_2O)(CO)Cu^+$–H_2O	17.4
$(CO)_2Cu^+$–H_2O	21.6

Similarly, the binding energy of water to $Cu^+(CO)$ (43.3 kcal/mol) is larger than the one to $Cu^+(H_2O)$ (40.2 kcal/mol). As expected, one can also observe a shortening of the metal–ligand distances in heteroleptic as compared to homoleptic complexes. Such an enhancement of the binding energies in di-coordinated gas phase species has already been observed [6] when the transition metal cation is simultaneously bound to a π-acceptor such as H_2 and a (weakly) π-donor such as H_2O. Such a thermodynamic effect is known in saturated organometallic species and referred to as "trans influence" or "static trans influence".

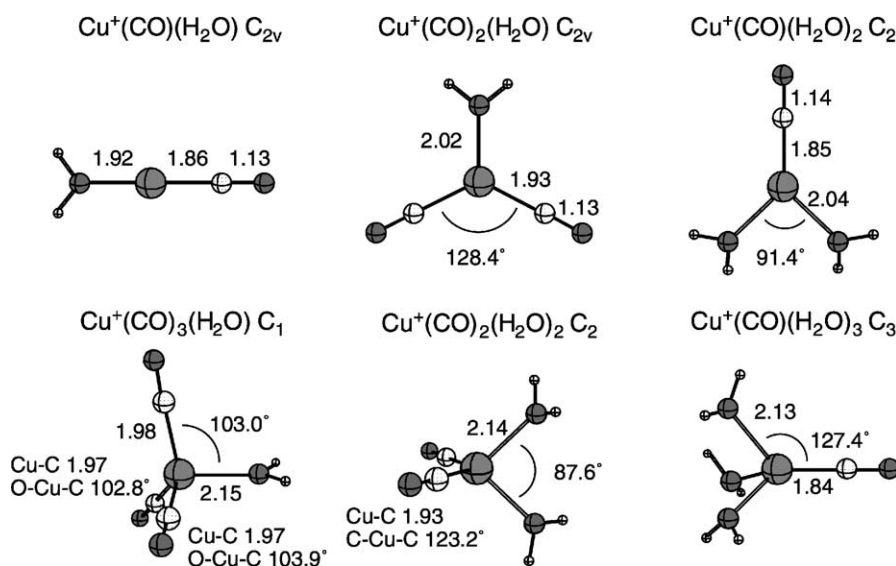Fig. 3. Complexes of $Cu^+(CO)_n(H_2O)_m$, $n + m = 1$–4. Distances are given in angstroms and angles in degrees.

The structure of the two heteroleptic tri-coordinated complexes derive from in-plane deformation from an ideal trigonal structure. $Cu^+(CO)_2(H_2O)$ adopts a T-shaped structure, but the distortion from the ideal trigonal structure is small since since the (CO)–Cu^+–(CO) angle is equal $128.4°$. The distortion is larger in the case of the Y-shaped structure of $Cu^+(CO)(H_2O)_2$, with an OCuO angle of $91.4°$. It is interesting to compare these structures to the ideal trigonal structures optimized with the imposing L–Cu^+–L angles at $120°$. In the case of $Cu^+(CO)_2(H_2O)$, the potential energy surface is essentially flat and the stabilization energy associated to the distortion from the ideal structure is only 0.25 kcal/mol. The corresponding stabilization energy in the case of $Cu^+(CO)(H_2O)_2$ is larger (1.9 kcal/mol) and, interestingly, it is associated to a substantial shortening (0.033 Å) of the Cu^+–CO distance. Preference for T-shaped vs. Y-shaped structure of tri-coordinated complexes can be rationalized by considering the interaction of the d-block metal orbitals with the π-ligand orbitals [35,36]. In particular, the shortening of the Cu^+–CO bond in $Cu^+(CO)(H_2O)_2$ can be analyzed as a reinforcement of the backdonation. Indeed, closing the (OH_2)–Cu^+–(OH_2) angle destabilizes a $3d_{Cu^+}$ orbital, and the destabilization is maximized for an angle close to $90°$ where the two water σ lone pairs maximize their overlap with the $3d_{Cu^+}$ orbital. This has the effect to reduce the energy gap between the in-plane π_{CO^*} and the symmetry adapted doubly occupied $3d_{Cu^+}$ orbital, and thus to reinforce the in-plane backdonation.

In the case of tetra-coordinated complexes (Fig. 3), one can also notice that the optimal structure of $Cu^+(CO)(H_2O)_3$ is strongly distorted from the ideal tetrahedral with a (CO)–Cu^+–(OH_2) angle of $127.4°$. As in the case of $Cu^+(CO)(H_2O)_2$, comparison with an ideal tetrahedral structure where all the parameters were optimized, except the L–Cu^+–L angles which were constrained to $109.47°$, reveals that the distortion from the ideal structure is associated to a stabilization energy of 5.3 kcal/mol and a shortening of the Cu^+–CO distance of 0.056 Å. As in the case of $Cu^+(CO)(H_2O)_2$ discussed above, the distortion from the ideal structure in $Cu^+(CO)(H_2O)_3$ seems to

be associated to a reinforcement of the Cu^+ to CO backdonation.

As can be seen in Table 3, our B3LYP/Basis2 results indicate that the binding energy of H_2O to $Cu^+(H_2O)(CO)$ (17.4 kcal/mol) and $Cu^+(CO)_2$ (21.6 kcal/mol) is much stronger than the one to $Cu^+(H_2O)_2$ (12.2 kcal/mol). On the contrary, binding energy of CO to $Cu^+(CO)_2$ (16.6 kcal/mol) is not strongly affected by the replacement of one (14.8 kcal/mol) or two (16.9 kcal/mol) CO by H_2O.

5. Analysis of the evolution of the binding energy with the cluster size

Bauschlicher and co-workers [26,28] gave evidences strongly suggesting that the Cu^+–OH_2 bonding scheme in the $Cu^+(H_2O)_n$ ($n = 1$–4) clusters is dominated by electrostatic, eventhough water to Cu^+ charge transfers occur. In particular, whereas the electronic correlation is essential to describe the bonding to a transition metal cation, they showed that at the Hartree–Fock level, which is well suited to describe the M^+–ligand electrostatic interactions, the essential features of the evolution of the binding energy with respect to the cluster size are well reproduced. On the contrary, in the case of the carbonyl clusters, the binding energy is significantly underestimated at the Hartree–Fock level using the same basis set (aug-cc-pVTZ on the ligands): 10.1, 14.0, 3.7 and 0.3 kcal/mol, as compared to 35.6, 41.1, 17.9 and 12.7 kcal/mol experimentally [25]. Despite these evidences for a very different bonding scheme between Cu^+–OH_2 and Cu^+–CO, it is interesting to note that the binding energy in the carbonyl and water clusters evolves the same way and that the sum for experimentally derived binding energies are comparable (107.3 kcal/mol for $Cu^+(CO)_4$ and 104.8 kcal/mol for $Cu^+(H_2O)_4$). That is, the average binding energy of Cu^+–CO in $Cu^+(CO)_4$ amounts to 26.8 kcal/mol while it is only slightly weaker (26.2 kcal/mol) in the case of water.

The origin of the fluctuation of the binding energy of a ligand as the cluster size increases has been

discussed [6,32], but with a special emphasis on the first two binding energies. The first studies on the di-coordinated species pointed out that the origin of the increase of the binding energy from the first to the second ligand was essentially due to a polarization of the metal. With the formation of the first bond to $Cu^+(d^{10})$ along the z-axis, calculations show that a $4s/3d_z^2$ hybridization occurs. That is, the doubly occupied $3d_z^2$ orbital evolves as a $4s$-$3d_z^2$ leading to a reduction of the electron density along the z-axis and to a simultaneous increase in the perpendicular plane. This hybridization allows for a closer approach of the ligand to the metallic center M^+, and thus an increase of the electrostatic interaction and a simultaneous reduction of the σ ligand–metal ($3d_z^2$) repulsion. The second effect of the hybridization is to polarize the $4s$ orbital along the z-axis ($4s + 3d_z^2$). This polarization of this empty orbital benefits to the ligand to metal charge transfer. Thence, assuming that the cost of the $4s$-$3d_z^2$ hybridization is essentially paid by the first ligand, the binding of the second ligand, approaching opposite to the first, is more favorable.

The large drop of the binding energy from the di- to the tri-coordinated complexes has been discussed in less details. In their work on the $Cu^+(H_2O)_n$ ($n = 1$–4) clusters [28], Bauschlicher et al. suggested that this decrease in the binding energy was due for two-thirds to ligand–ligand repulsion, the rest being the result of the loss of the sd_σ hybridization. This conclusions were based in particular on model calculations where the Cu^+ was replaced by a point charge. Interestingly, the evolution of the binding energy to Cu^+ is very similar in the case of H_2O and H_2, a large drop of the binding energy being observed with the addition of the third ligand. Considering the smaller size of H_2 than H_2O, it was interesting to evaluate the contribution of the ligand–ligand repulsion. This had been examined in the case of $Cu^+(H_2)_n$ ($n = 1$–4) clusters [6]. Not surprisingly, the ligand–ligand repulsion was shown to be negligible in these dihydrogen clusters. It was rather suggested that the diminution of the binding energy essentially correlates to the σ metal–ligand repulsion increase. In order to analyze this repulsion between σ electrons, one can consider an ideal planar

trigonal geometry (D_{3h}) for the tri-coordinated Cu^+ complex. The symmetry of the metal orbitals are a_1' for the $4s$ and $a_1' + e' + e''$ for the $3d$. Since the symmetry of the three donating orbitals of the ligands are $a_1' + e'$, three $3d$ orbitals ($a_1' + e'$) are destabilized as the result of the metal–ligand σ repulsion. Since the a_1' σ-orbital of the ligands interacts with both the $4s$ and the $3d_z^2(a_1')$ orbital, a sd_σ hybridization occurs, reducing the repulsion with the $3d_z^2(a_1')$ orbital through a polarization along the z-axis perpendicular to the molecular plane. Another σ-repulsion occurs through the interaction of the e' type orbitals. That is, the two degenerate and doubly occupied $3d_{x^2-y^2}$ and $3d_{xy}$ are destabilized by the two e' σ-orbital of the ligands. In principle, $3d$-$4p$ hybridization could reduce the destabilization of the $3d(e')$ orbitals as the $3d$-$4s$ hybridization reduces the destabilization of the $3d_z^2(a_1')$. Nevertheless, population analysis shows that the $4p$ orbitals of first-row metal cations do not participate to the bonding scheme. That is, while only two $3d$ electrons are destabilized by metal–ligand σ-repulsion in the two first complexes, the addition of the third ligand destabilizes two extra pairs of $3d$ electrons. This increase of the metal–ligand σ-repulsion contributes to the diminution of the metal–ligand binding energy. The effect of the addition of the fourth ligand to the metal cation can be simply understood assuming an ideal tetrahedral geometry. In this symmetry point group, the $4s$ orbital is a_1, and the $3d$ orbitals are $e + t_2$, that is no $4s$-$3d$ hybridization can occur. The three $3d$ orbitals which are destabilized by the σ-donating orbitals of the ligands are t_2 type, and sd hybridization cannot occur for symmetry reason. The symmetry of the four donating orbitals of the ligands are $a_1 + t_2$. That is, three doubly occupied $3d$ orbitals are destabilized by the ligands and no hybridization scheme can reduce this metal–ligand σ-repulsion. Since no sd_σ hybridization occurs in the tetra-coordinated complex, the average value of the binding energy in the tetra-coordinated cluster is the binding energy that could be expected without polarization of the metal cation. In the cases of H_2, CO and H_2O, the values derived from experiments are 11.5, 26.8, 26.2 kcal/mol, respectively.

The π-type interactions, backdonation in the case of H_2 and CO and (weak) donation in the case of water, might also play a role. Nonetheless, if one expresses the successive binding energy as a percentage with respect to the average binding in the tetra-coordinated cluster, one can notice that the variations in the cases of $Cu^+(H_2)_n$ (+34, +45, −23 and −56%) and $Cu^+(CO)_n$ (+32, +53, −33 and −53%) are very similar for the two π-acceptor ligands H_2 and CO. This similarity between the two π-acceptor ligands CO and H_2 has already been noticed [6]. The evolution of the binding energy in the case of $Cu^+(OH_2)_n$ (+44, +58, −48 and −50%) slightly differs from the two other systems, the first BDE being 44% greater than the average value (+34 and +32% in the case of $Cu^+(H_2)_1$ and $Cu^+(CO)_1$, respectively) and the third BDE being −48% smaller than the average value (−23% and −33% in the case of $Cu^+(H_2)_3$ and $Cu^+(CO)_3$, respectively). The fact that the drop in binding energy between the di- and the tri-coordinated clusters is smaller in the case of π-acceptor ligands than in the case of H_2O could be interpreted in terms of an alternative reduction of the metal–ligand repulsion. As said above, the 3d-4p hybridization is inefficient to reduce the destabilization of the 3d(e') orbitals in an ideal planar trigonal complex. Nevertheless, this destabilization of these two degenerate 3d orbitals can benefit to the backdonation in the tri-coordinated complexes since it reduces the energy difference with the π-acceptor orbitals and thus increases the backdonation. This "push-pull" mechanism has the effect of simultaneously reducing σ-repulsion and increasing the backdonation in tri-coordinated π-acceptor containing complexes.

6. Competition between simple substitution and cluster-assisted reactions

As mentioned in the introduction, experiments were only performed in the case of Fe^+ complexes, and Cu^+ complexes have been chosen as models of late first-row transition metal cations. Indeed, we think that the trends observed experimentally are essen-

tially due to the evolution of the metal–ligand binding energy with respect to the coordination number n, and in particular to the dramatic breakdown observed when going from $n = 2$ to 3 which is observed for all the late first-row transition metal cations.

Using the Fourier transform ion cyclotron resonance mass spectrometry (FT-ICR-MS) technique, the following trends were observed: when $Fe^+(CO)_n$ complexes are allowed to react with L = H_2O, CH_3OH and CH_3OCH_3 in an ICR cell, substitutions of CO by L are observed. While in the case of $Fe^+(CO)_n$ ($n = 1, 2$) complexes the substitution is complete, one CO remains unsubstituted when the ion complexes are $Fe^+(CO)_3$ and $Fe^+(CO)_4$. One could expect that the relative strength of CO and oxygen-donor ligand with Fe^+ changes as a function of the substitution reaction, the CO becoming more strongly bound to Fe^+ than the oxygen-donor ligands in the $Fe^+(CO)L_2$ and $Fe^+(CO)L_3$ clusters. An alternative interpretation would be that a condensation reaction occurs between CO and an oxygen-donor ligand in the coordination sphere of the metal cation.

In order to evaluate the performance of B3LYP/ Basis2, we compared our results to the available experimental data concerning the reaction between neutrals. Experimentally, formation of methanoic acid from H_2O + CO is known to be exothermic by −6.3 kcal/mol at 298 K [37]. An "experimental" value of −4.4 kcal/mol for the reaction enthalpy at 0 K was derived by using the calculated thermal contributions. The calculated reaction enthalpy at 0 K at the B3LYP/Basis2 level of theory was found to be −7.5 kcal/mol. Thence, one can notice that this level of calculation intrinsically slightly overestimates the exothermicity of the formation of methanoic acid from H_2O + CO by about 3 kcal/mol.

Reaction enthalpies associated to the successive substitution reactions of CO by water from $Cu^+(CO)_n$ clusters are reported in Table 4. While the successive substitutions of CO by water are exothermics from mono- and di-carbonyl complexes, the last substitution of CO from the tri- and tetra-carbonyl complexes is endothermic. This would support the first interpretation of the exchange reactions of CO

Table 4

Reaction enthalpy at 0 K (kcal/mol) evaluated at the B3LYP/Basis2 level, for the successive substitution reactions of CO by H_2O from $Cu^+(CO)_n$, $n = 1–4$

n	Substitution reactions	$\Delta_r H$
1	$Cu^+(CO) + H_2O \rightarrow Cu^+(H_2O) + CO$	−3.6
2	$Cu^+(CO)_2 + H_2O \rightarrow Cu^+(CO)(H_2O) + CO$	−6.8
	$Cu^+(CO)(H_2O) + H_2O \rightarrow Cu^+(H_2O)_2 + CO$	−0.6
3	$Cu^+(CO)_3 + H_2O \rightarrow Cu^+(CO)_2(H_2O) + CO$	−5.0
	$Cu^+(CO)_2(H_2O) + H_2O \rightarrow Cu^+(CO)(H_2O)_2 + CO$	−2.6
	$Cu^+(CO)(H_2O)_2 + H_2O \rightarrow Cu^+(H_2O)_3 + CO$	+4.6
4	$Cu^+(CO)_4 + H_2O \rightarrow Cu^+(CO)_3(H_2O) + CO$	−3.8
	$Cu^+(CO)_3(H_2O) + H_2O \rightarrow Cu^+(CO)_2(H_2O)_2 + CO$	−2.5
	$Cu^+(CO)_2(H_2O)_2 + H_2O \rightarrow Cu^+(CO)(H_2O)_3 + CO$	−0.7
	$Cu^+(CO)(H_2O)_3 + H_2O \rightarrow Cu^+(H_2O)_4 + CO$	+8.9

by oxygen-donor ligands starting from $Fe^+(CO)_n$ ($n = 1–4$) clusters. That is, oxygen-donor ligands $L = H_2O$, CH_3OH and CH_3OCH_3 are more strongly bound than CO, except in the case of the $Fe^+(CO)L_2$ and $Fe^+(CO)L_3$ clusters, which would explain that substitution reactions of CO by L do not occur from these two clusters. This result could be interpreted based on the discussion of the distortion of the $Cu^+(CO)(H_2O)_2$ and $Cu^+(CO)(H_2O)_3$ from the ideal trigonal and tetrahedral geometry, respectively

(Section 4). We showed that the distortion from the ideal structures is accompanied by a shortening of the Cu^+–CO distance which would be consistent with a increase of the Cu^+ to CO backdonation, and thus to an increase of the Cu^+–CO bond strength.

Alternatively, the lack of substitution reaction of CO by L from the $Fe^+(CO)L_2$ and $Fe^+(CO)L_3$ complexes could owe its origin to an intracluster condensation reaction between CO and an oxygen-donor ligand. In order to test this hypothesis, thermodynamic of the formation of methanoic acid from H_2O + CO in the coordination sphere of Cu^+ has been evaluated. The different optimized structures for HCOOH-containing copper complexes, all corresponding to minima, are depicted in Fig. 4. Reaction enthalpies corresponding to the formation of HCOOH acid from CO and H_2O in the coordination sphere of Cu^+ are given in Table 5. In order to facilitate the comparison, we considered the same type of stoichiometry as with substitution reactions, i.e., with a H_2O molecule as neutral reactant and a CO molecule as neutral product. The expected trend in the condensation reaction enthalpies was found. That is, formation of methanoic acid in the coordination sphere of Cu^+ from H_2O + $Cu^+(CO)_2$ is very endothermic, and becomes more favorable from
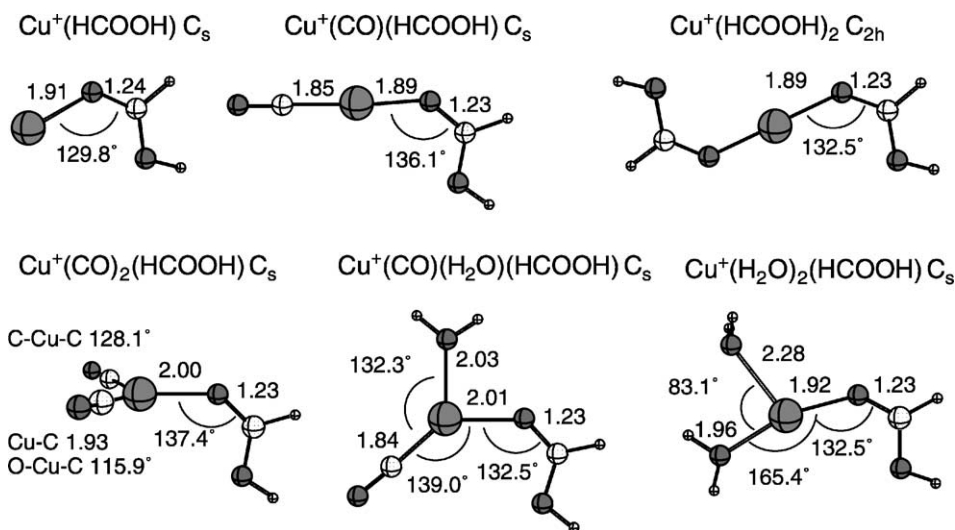

Fig. 4. Structures for complexes of $Cu^+(HCOOH)(CO)_n(H_2O)_m$, $m + n = 0–2$, and of Cu^+ $(HCOOH)_2$. Distances are given in angstroms and angles in degrees.

Table 5
Reaction enthalpy at 0 K (kcal/mol) evaluated at the B3LYP/Basis2 level for the formation of methanoic acid from CO and water

n	Reactions	$\Delta_r H$
2	$Cu^+(CO)_2 + H_2O \rightarrow Cu^+(HCOOH) + CO$	19.5
3	$Cu^+(CO)_3 + H_2O \rightarrow Cu^+(HCOOH)(CO) + CO$	−2.6
	$Cu^+(CO)_2(H_2O) + H_2O \rightarrow Cu^+(HCOOH)(H_2O) + CO$	3.2
4	$Cu^+(CO)_4 + H_2O \rightarrow Cu^+(HCOOH)(CO)_2 + CO$	−3.2
	$Cu^+(CO)_3(H_2O) + H_2O \rightarrow Cu^+(HCOOH)(H_2O)(CO) + CO$	−2.1
	$Cu^+ (CO)_2(H_2O)_2 + H_2O \rightarrow Cu^+(HCOOH)(H_2O)_2 + CO$	7.5

Table 6
Successive reactions of $Cu^+(CO)_n$, $n = 1–3$ with methanol: enthalpy at 0 K (kcal/mol) evaluated at the B3LYP/Basis2 level

n	Reactants	Substitution		Condensation/substitution	
		Ionic product	$\Delta_r H$	Ionic product	$\Delta_r H$
1	$Cu^+(CO) + CH_3OH$	$Cu^+(CH_3OH)$	−8.6	–	
2	$Cu^+(CO)_2 + CH_3OH$	$Cu^+(CO)(CH_3OH)$	−11.2	$Cu^+(CH_3COOH)$	−7.1
	$Cu^+(CO)(CH_3OH) + CH_3OH$	$Cu^+(CH_3OH)_2$	−4.3	–	
3	$Cu^+(CO)_3 + CH_3OH$	$Cu^+(CO)_2(CH_3OH)$	−9.0	$Cu^+(CO)(CH_3COOH)$	−28.1
	$Cu^+(CO)_2(CH_3OH) + CH_3OH$	$Cu^+(CO)(CH_3OH)_2$	−5.8	$Cu^+(CH_3OH)(CH_3COOH)$	−22.7
	$Cu^+(CO)(CH_3OH)_2 + CH_3OH$	$Cu^+(CH_3OH)_3$	+3.2	–	

For all reactions the neutral product is CO.

$H_2O + Cu^+(CO)_3$ and $H_2O + Cu^+(CO)_4$. Compared to the simple substitution reactions (Table 4), these condensation reactions are less favorable since we have seen above that the exothermicity of $H_2O + CO$ is intrinsically overestimated by 3 kcal/mol.

The same calculations with methanol instead of water have been performed, but we restricted ourselves to mono-, di- and tri-coordinated complexes. The intracluster reaction between CO and CH_3OH ligands can conceivably lead to methyl formate $HCOOCH_3$, or ethanoic acid CH_3COOH. We restricted to the latter, which is more exothermic than the latter (24 kcal/mol vs. 12 kcal/mol). In the case of methanol, condensation reaction with CO leading to the formation of ethanoic acid is more exothermic than in the case of water since the corresponding reaction enthalpy at 0 K can be estimated to be −24.1 kcal/mol from the experimental value at 298 K [37]. As for the formation of methanoic acid from water and carbon monoxide, the exothermicity of the formation of ethanoic acid is overestimated by 4.4 kcal/mol in the present case. In Table 6, we give

the enthalpies determined for the substitution reactions of CO by CH_3OH from $Cu^+(CO)_{n−m}(CH_3OH)_m$ ($n = 1–3$, $m \leq n$) and the one of the corresponding competing condensation reaction. The same trends as for water can be observed. When the substitution reactions are considered, the substitution of CO by methanol is less and less favorable when the number of methanol m increases for $n = 2$ and 3. Moreover, as in the case of water, calculations suggest that substitution of CO by CH_3OH from $Cu^+(CO)_1(CH_3OH)_2$ would not occur. Condensation reactions are more favorable in the case of methanol than in the case of water, which is expected since the former is intrinsically more favorable than the latter (−24.1 kcal/mol vs. −3.3 kcal/mol experimentally).

7. Concluding remarks

In order to cover homoleptic and heteroleptic Cu^+ complexes of different sizes bearing various ligands,

i.e., complexes of CO, H_2O, CH_3OH, HCOOH with coordination numbers $n = 1$–4, a suitable method had to be found for quantum chemical calculations. Among the different methods tested, B3LYP appeared to be the most reliable one, providing the use of a large enough basis set. These quantum chemical calculations have allowed to predict trends relative to the thermochemistry of the successive ligand substitution of CO by H_2O of Cu^+ complexes. As the coordination of Cu^+ increases, beside the simple substitution reaction, a condensation reaction of $CO + H_2O$ might compete. The reactivity is much more favorable in tri- and tetra-coordinated complexes than in mono- and di-coordinated species, and this can be simply interpreted from the known evolution of the binding energy to Cu^+ as a function of coordination number.

The trends observed in the case of the model Cu^+ complexes can be generalized to the other late transition metal cations M^+ of the first row. Indeed, for all these cations, it has been shown that due to a dramatic increase of the σ metal–ligand repulsion with the addition of the third ligand to M^+, the evolution of the binding energy to M^+ as a function of the coordination number shows a significant decrease when going from the second to the third ligand. As a consequence, Feller et al. [29] have shown that it is energetically preferable to form a hydrogen bond between H_2O and $Cu(OH_2)_2{}^+$ rather than forming a tri-coordinated $Cu(OH_2)_3{}^+$ complex. In this paper, we show that from a thermodynamic point of view, the direct coordination of ROH to $Cu^+(CO)_{n-m}(ROH)_m$ ($m \leq n$) could be less favorable than the condensation reaction leading to $Cu^+(RC(O)OH)(CO)_{n-m-1}(ROH)_{m-1}$ for R = H or CH_3. These results could be interesting to rationalize the trends experimentally observed on Fe^+ complexes [9–11]: successive substitutions of CO by water molecules from $Fe^+(CO)_n$, for example, have been observed except in the case of $n = 3$ and 4, where the one CO remains unsubstituted. Thus, one could think that the successive substitutions of CO by water molecules from $Fe^+(CO)_3$ and $Fe^+(CO)_4$ lead to the terminal ions $Fe^+(HC(O)OH)(H_2O)$ and $Fe^+(HC(O)OH)(H_2O)_2$, respectively, which could explain that the last "CO" remains unsubstituted. Al-

ternatively, if $Fe^+(CO)(H_2O)_2$ and $Fe^+(CO)(H_2O)_3$ are the terminal ions formed, the calculated binding energies of H_2O and CO to Fe^+ in these complexes show that the last CO should remain unsubstituted. Finally, we should point out that the present study on Cu^+ complexes only aims at suggesting the favorable thermodynamic of intracluster condensation reaction in Fe^+ complexes. However, a complete elucidation of this question would require the knowledge of the corresponding activation barriers. Quantum chemical calculations are currently undertaken in the case of iron complexes in order to characterize the transition states.

It has already been noticed that bisligated complexes play a special role in the chemistry of Cu^+. Luna et al., for instance, showed that the precursors of the fragmentation of Cu^+-urea [38], Cu^+-formamide [39], and Cu^+-guanidine [40] are systematically di-coordinated species. The particular stability of di-coordinated complexes could also be the driving force to intracluster bond-forming reactions in the heteroleptic complexes in the present work.

Interplay between FT-ICR-MS experiments and quantum chemical calculations have been shown to be particularly helpful, especially for the characterization of the structure of the ions. With this respect, our recent development of an experimental set-up featuring the coupling of our mobile FT-ICR ion trap (MICRA) with the Orsay free electron laser (CLIO) [41], allowing for a direct structural characterization of ions in the gas phase through infrared spectroscopy is an interesting perspective and the tri- and tetra-coordinated heteroleptic iron complexes are under study.

Acknowledgements

References

[1] K. Eller, H. Schwarz, Chem. Rev. 91 (1991) 1121.
[2] L. Capron, H. Mestdagh, C. Rolando, Coord. Chem. Rev. 178–180 (1998) 269.

[3] C.W. Bauschlicher Jr., S.R. Langhoff, H. Partridge, in: B.S. Freiser (Ed.), Organometallic Ion Chemistry, Kluwer Academic Publishers, Dordrecht, 1996, p. 47.

[4] S.S. Yi, M.R.A. Blomberg, P.E.M. Siegbahn, J.C. Weisshaar, J. Phys. Chem. A 102 (1998) 395.

[5] H. Schwarz, D. Schroder, Pure Appl. Chem. 72 (2000) 2319.

[6] P.R. Kemper, P. Weis, M.T. Bowers, P. Maître, J. Am. Chem. Soc. 120 (1998) 13494.

[7] J.B. Schilling, W.A. Goddard III, J.L. Beauchamp, J. Am. Chem. Soc. 108 (1986) 582.

[8] J.B. Schilling, W.A. Goddard III, J.L. Beauchamp, J. Phys. Chem. 91 (1987) 5616.

[9] S. Le Caër, M. Heninger, H. Mestdagh, Chem. Phys. Lett. 352 (2002) 393.

[10] M. Heninger, P. Pernot, H. Mestdagh, P. Boissel, J. Lemaire, R. Marx, G. Mauclaire, Int. J. Mass Spectrom. 199 (2000) 267.

[11] S. Le Caër, M. Heninger, P. Pernot, H. Mestdagh, Phys. Chem. Chem. Phys. 4 (2002) 1855.

[12] A.J.H. Wachters, J. Chem. Phys. 52 (1970) 1033.

[13] C.W. Bauschlicher Jr., Theoretica Chimica Acta 92 (1995) 183.

[14] T.H. Dunning, J. Chem. Phys. 90 (1989) 1007.

[15] J.S. Krishnan, J.S. Binkley, P.V.R. Seeger, J.A. Pople, J. Chem. Phys. 72 (1980) 650.

[16] R.A. Kendall, T.H. Dunning, R.J. Harrison, J. Chem. Phys. 96 (1992) 6796.

[17] A.D. Becke, J. Chem. Phys. 98 (1993) 5648.

[18] A. Luna, M. Alcami, O. Mo, M. Yanez, Chem. Phys. Lett. 320 (2000) 129.

[19] P.J. Stephens, F.J. Devlin, C.F. Chabalowski, M.J. Frisch, J. Phys. Chem. A 98 (1994) 11623.

[20] P.J. Knowles, C. Hampel, H.-J. Werner, J. Chem. Phys. 99 (1993) 5219.

[21] J.D. Watts, J. Gauss, R.J. Bartlett, J. Chem. Phys. 98 (1993) 8718.

[22] MOLPRO is a package of ab initio programs written by H.-J. Werner, P.J. Knowles with contributions from R.D. Amos, A. Bernhardsson, A. Berning, P. Celani, D.L. Cooper, M.J.O. Deegan, A.J. Dobbyn, F. Eckert, C. Hampel, G. Hetzer, T. Korona, R. Lindh, A.W. Lloyd, S.J. McNicholas, F.R. Manby, W. Meyer, M.E. Mura, A. Nicklass, P. Palmieri, R. Pitzer, G. Rauhut, M. SchŸtz, H. Stoll, A.J. Stone, R. Tarroni, T. Thorsteinsson.

[23] G.W.T.M.J. Frisch, H.B. Schlegel, G.E. Scuseria, M.A. Robb, J.R. Cheeseman, V.G. Zakrzewski, J.A. Mongomery, R.E. Stratmann, J.C. Burant, S. Dapprich, J.M. Millam, A.D. Daniels, K.N. Kudin, M.C. Strain, O. Farkas, J. Tomasi, V. Barone, M. Cossi, R. Cammi, B. Mennucci, C. Pomelli, C. Adamo, S. Clifford, J. Ochterski, G.A. Petersson, P.Y. Ayala, Q. Cui, K. Morokuma, D.K. Malik, A.D. Rabuck, K. Raghavachari, J.B. Foresman, J. Ciolowski, J.V. Ortiz, B.B. Stefanov, G. Liu, A. Liashenko, P. Piskorz, I. Komaromi, R. Gomperts, R.L. Martin, D.J. Fox, T. Keith, M.A. Al-Laham, C.Y. Peng, A. Nanayakkara, C. Gonzales, M. Challacombe, P.M.W. Gill, B.G. Johnson, W. Chen, M.W. Wong, J.L. Andres, M. Head-Gordon, E.S. Replogle, J.A. Pople, Gaussian 98, Gaussian Inc., Pittsburgh, 1998 (1995).

[24] T.F. Magnera, D.E. David, J. Michl, J. Am. Chem. Soc. 111 (1989) 4100.

[25] N.F. Dalleska, K. Honma, L.S. Sunderlin, P.B. Armentrout, J. Am. Chem. Soc. 116 (1994) 3519.

[26] M. Rosi, C.W. Bauschlicher Jr., J. Chem. Phys. 90 (1989) 7264.

[27] M. Rosi, C.W. Bauschlicher Jr., J. Chem. Phys. 92 (1990) 1876.

[28] C.W. Bauschlicher Jr., S.R. Langhoff, H. Partridge, J. Chem. Phys. 94 (1991) 2068.

[29] D. Feller, E.D. Glendening, W.A.D. Jong, J. Chem. Phys. 110 (1999) 1475.

[30] A. Ricca, C.W. Bauschlicher Jr., J. Phys. Chem. 98 (1994) 12899.

[31] F. Meyer, Y.M. Chen, P.B. Armentrout, J. Am. Chem. Soc. 117 (1995) 4071.

[32] L.A. Barnes, M. Rosi, C.W. Bauschlicher Jr., J. Chem. Phys. 93 (1990) 609.

[33] J.M.L. Martin, Chem. Phys. Lett. 259 (1996) 669.

[34] A. Ricca, Chem. Phys. Lett. 350 (2001) 313.

[35] I.E.-I. Rachidi, O. Eisenstein, Y. Jean, New J. Chem. 14 (1990) 671.

[36] J.F. Riehl, Y. Jean, O. Eisenstein, M. Pélissier, Organometallics 11 (1992) 729.

[37] Handbook of Chemistry and Physics, CRC Press, Boca Raton, 1992/1993.

[38] A. Luna, B. Amekraz, J.P. Morizur, J. Tortajada, O. Mo, M. Yanez, J. Phys. Chem. A 104 (2000) 3132.

[39] A. Luna, B. Amekraz, J. Tortajada, J.P. Morizur, M. Alcami, O. Mo, M. Yanez, J. Am. Chem. Soc. 120 (1998) 5411.

[40] A. Luna, B. Amekraz, J.P. Morizur, J. Tortajada, O. Mo, M. Yanez, J. Phys. Chem. A 101 (1997) 5931.

[41] J. Lemaire, P. Boissel, M. Heninger, G. Mauclaire, G. Bellec, H. Mestdagh, A. Simon, S. Le Caër, F. Glotin, J.M. Ortega, P. Maître, Phys. Rev. Lett. 89 (2002) 273002.